

Combustion of oxygenated biofuels in flames

Pierre-Alexandre Glaude

Laboratoire Réaction et Génie des Procédés, CNRS – Université de Lorraine,
1 rue Grandville, 54000 Nancy, France.

ABSTRACT

An increasing interest is noted to shift from fossil fuels to bio-fuels. The use of bio-fuels allows a reduction of the dependence on petroleum-based fuels. Moreover burning bio-fuel should not lead to an increase of the total amount of greenhouse gases in the atmosphere. The study of the structure of premixed laminar flames of hydrocarbons and oxygenates makes it possible to know the reactivity of these compounds and to follow the formation of intermediates and reaction products in the flame front. Flames of several saturated cyclic ethers, such as tetrahydrofuran, methyltetrahydrofura and tetrahydropyran, and alcohols, such as 1-pentanol, were investigated under low pressure using argon as a diluent. The reaction products were sampled by a microprobe and analyzed on-line by different chromatographs, which made it possible to quantify a large number of stable species. Besides the structure, the flame velocity is a key parameter for the design of burners and combustion chambers. A heat flux burner was developed and used to measure the adiabatic laminar flame velocities of liquid hydrocarbons and oxygenates as a function of the richness and temperature of the fresh gases.

Keywords

Laminar premixed flame, burning velocity, bio-fuels, cyclic ethers, combustion chemistry.

Corresponding author: pierre-alexandre.glaude@univ-lorraine.fr

Laboratoire Réaction et Génie des Procédés

CNRS – Université de Lorraine

1 rue Grandville, 54000 Nancy, France

Tel.: +33372743821

Book of Abstracts of the 9th International Seminar on Flame Structure
and First Young Researchers' School on Flame Study

INTRODUCTION

More than 90% of the liquid fuels consumed in the world for transportation are derived from petroleum. Possible scarcity of the resource in the long term and the need to reduce greenhouse gas emissions have led to growing interest in fuels produced from renewable vegetal matter. The first generation of biofuels, such as ethanol or methyl esters of fatty acids suffer from the limitation of resources and of the competition with food crops. Second-generation biofuels, derived from ligno-cellulosic biomass, i.e. derived from non-edible raw materials, are preferable for the reduction of greenhouse gases since the whole plant would be used, and for the reliability of the feedstock. According to the chemical process, these fuels can be alkanes, alcohols or ethers, which are produced via synthesis gas, or saturated or unsaturated cyclic ethers, such as derivatives of furan and tetrahydrofuran. Another interest in the addition of oxygen-containing compounds to fuels lies in their ability to reduce soot formation in diesel engines, but in some cases offset by increased emissions of toxics or irritants, such as aldehydes.

Alcohols such as butanols or pentanols and cyclic ethers such as tetrahydrofuran and tetrahydropyran family, e.g. 2-methyltetrahydrofuran, (MTHF) 2,5-dimethyltetrahydrofuran (DMTHF) have been considered as promising bio-fuel compounds for adding to gasoline fuel. They have a lower heating value (~28.5-29.5 MJ/L), which is close to that of furan family fuels (~27.7-30.0 MJ/L) and of gasoline (~31.6MJ/L), and higher than that of ethanol (~21.3 MJ/L). MTHF has good antiknock characteristics, and satisfactory performance when mixed in a 10% blend with gasoline in conventional internal combustion engine [1]. The cyclic ethers fuels can be produced from non-edible biomass [2][3][4]. Up to 25% of 1-pentanol was successfully blended with diesel fuel in engine [5][6]. Some tests for MTHF on engine have been also reported. Rudolph and Thomas [7] have comparatively analyzed pollutant emissions from a spark-ignition engine performed on mixtures of gasoline with 10% potential liquid fuels, including ethanol, methanol, methyl t-butyl ether (MTBE), and MTHF. The result has shown that the fuel blend containing 10% MTHF has power outputs and carbon monoxide, nitrogen oxides, and non-methane hydrocarbons emissions that most closely resemble unleaded gasoline. Furthermore, THF, MTHF, DMTHF, THP and other saturated cyclic ethers have been also identified among the emissions produced during the combustion and auto-ignition of alkanes and alkenes by isomerization of alkylhydroperoxy radicals [8][9][10]. The subsequent reactions of these cyclic ethers can then influence the overall chemical kinetics mechanisms of alkanes and alkenes combustion. The structure of the cyclic ethers is displayed in figure 1.

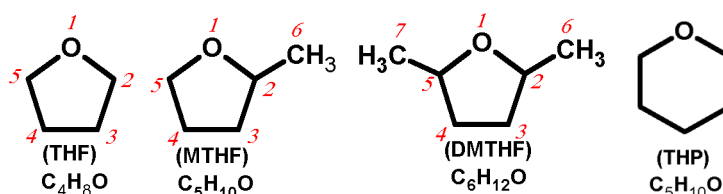


Figure 1. Structure of saturated cyclic ethers

The fundamental understanding of their combustion chemistry is really wishful. THF is well suited as a model fuel to study the combustion chemistry of saturated cyclic ethers, especially of its derivatives. Very early, the pyrolysis of THF has been studied [11][12][13]. The later suggested two main possible decomposition pathways of THF which give: (i) ethylene and $(\text{CH}_2)_2\text{O}$ bi-radical, and (ii) propene and formaldehyde with a rate constant of four times lower than the first one. The low-temperature oxidation of THF has been investigated by Molera et al. [14], in a static reactor. A motored engine study on auto-ignition chemistry of acyclic and cyclic ethers, including MTBE, ethyl t-butyl ether-ETBE, methyl t-amyl ether-TAME, THF, MTHF, and THP, has been performed by Leppard [15]. The chemical mechanisms responsible for auto-ignition of both ether classes are detailed, compared, and used to explain the differences in antiknock characteristics of the two ether classes. The author explained that, due to a dominance of very reactive alkoxy-carbonyl radicals produced by low temperature oxygen-addition chemistry in the cyclic ethers auto-ignition, octane number of the cyclic ethers is significantly lower than that of acyclic ethers. Later, the ignition delay times and oxidation of THF have been studied in a single-pulse shock tube and in a jet-stirred reactor, respectively, under a range of conditions of 202-1013 kPa, $0.5 \leq \phi \leq 2.0$, 800-1800 K [16]. This study has shown that a large amount of aldehydes (formaldehyde, acetaldehyde, and propanal) were produced during the THF oxidation. Recently, Kasper et al. [17] investigated the structure of laminar premixed low-pressure THF flames using photoionization (PI) and electron-ionization (EI) molecular-beam mass spectrometry (MBMS). About 60 intermediates were measured and analyzed, but several assumptions have been given for species identification. Large uncertainties in mole fraction values were considered, especially for minor species, and some species assignment remained ambiguous and uncertain. The kinetics and thermochemistry of saturated cyclic ethers have been theoretically investigated by Simmie [18], while theoretical studies focused on their initial decomposition steps [19][20]. In the case of the linear C_5 alcohol, the auto-ignition delay times of 1-pentanol were determined in shock tube and rapid compression machine [21][22]. Detailed speciation of oxidation products was obtained in a JSR, which allow the validation of a detailed chemical kinetic model [23]. Laminar burning velocity were evaluated from spherical explosion vessel experiments [23][24]. Eventually, Zhao et al. [25] investigated theoretically the thermal decomposition of 1-pentanol.

The above bibliography shows the scarcity of data about the combustion of saturated cyclic ethers and alcohols larger than ethanol and butanols in laminar premixed low-pressure flame as well as in other fundamental devices, which provide a stringent test for kinetic reaction models. The present work, as part of a continuing effort to enrich experimental data and to improve the knowledge on the combustion chemistry of oxygenated fuels, compares experimental data of stoichiometric low-pressure premixed THF, MTHF, THP, and pentanol flames diluted in argon, using on-line gas chromatography analyses. Moreover, laminar burning velocity in air were determined in a heat flux burner.

EXPERIMENTAL METHODS

Low pressure flat flame

The experimental setup has been developed to study stable species profiles in a laminar premixed flat flame at low-pressure and has been described previously [26]. Briefly, all flames were stabilized on a McKenna burner (diameter 60 mm, water-cooled) housed in a vacuum chamber which is maintained at 50 Torr. The burner is cooled with water at a constant temperature of 333 K. Oxygen (99.5% pure) and argon (99.995% pure) were provided by Messer. Liquid fuels: THF (>99.7 % pure) and MTHF (>99.0 % pure) and THP (>98% pure), were supplied by VWR, Sigma-Aldrich, and Alfa Aesar respectively. Liquid fuel was contained in a metallic vessel pressurized with argon. After each load of liquid fuel, argon bubbling and vacuum pumping were performed in order to remove traces of dissolved gases. Liquid fuel was mixed with argon and then evaporated by passing through a Controlled Evaporator and Mixer (CEM). The temperature of this CEM was set at 373 K. Liquid and gas flow rates were measured by using mass flow controllers provided by Bronkhorst, with a mass flow accuracy of 0.5%.

Analyses were made by GC with a heated (423 K) online connection to a quartz probe. The quartz probe had an upper diameter of 6 mm and was tipped by a small cone with a 100 μm diameter orifice at the tip and an angle to the vertical of 22°. Three types of columns were used: Carbosphere, HP-Molsieve, and HP-Plot Q, and two types of detectors: flame ionization detection (FID) coupled with a methanizer and thermal conductivity detection (TCD). The Carbosphere column with argon as carrier gas was used to analyze O_2 and H_2 by TCD. The HP-Molsieve column with helium as carrier gas was used to analyze CH_4 and C_2H_4 by FID and Ar by TCD. The HP-Plot Q column with helium as carrier gas was used to analyze all hydrocarbon species from C_2 and oxygenated species by FID. Additionally, this column was used also to analyze H_2O by TCD. Usually in GC, CO and CO_2 can only be detected by TCD, and formaldehyde cannot be measured by FID. Here, CO, CO_2 , as well as formaldehyde, were converted to methane by passing through a methanizer, and could then be detected by FID which is more sensitive (by a factor of 100) than TCD. Stable species were identified by the determination of their individual retention times and by mass spectrometry (GC/MS). Calibrations were made directly using cold-gas mixtures. The calibration factors were estimated using the effective carbon number method for species for which a direct calibration procedure was not possible. The calculated uncertainties of the mole fraction measurements of the quantified species were ~5% for the major compounds and ~10% for minor products (<100 ppm). The FID detection threshold was about 0.5 ppm, while the TCD detection limit was about 50 ppm for H_2O , H_2 and O_2 . Flames of THF, MTHF, and THP, and pentanol were investigated under the same conditions, pressure of 50 Torr with a dilution of 78 %, a gas velocity of 69 cm s^{-1} at 333 K, and stoichiometric mixtures. The initial operating conditions of these flames are presented in Table 1.

Table 1. Flame conditions

Flame name	ϕ	Gas flow (NL/min)			C/O	C/H	Pressure (Torr)	Dilution* (%)
		Fuel	O_2	Ar				
THF	1.0	0.234	1.29	4.56	0.33	0.5	50	78
MTHF	1.0	0.187	1.31	4.64	0.33	0.5	50	78
THP	1.0	0.187	1.31	4.64	0.33	0.5	50	78

1-Pentanol	1.0	0.18	1.31	4.64	0.32	0.42	50	78
------------	-----	------	------	------	------	------	----	----

*Dilution=Ar/(Ar+O₂); φ-equivalence ratio.

Heat flux burner

The measurements of laminar burning velocities were performed using the same atmospheric pressure heat flux burner as that used to study components of natural gas [27] and gasoline [28][29]. The heat flux method proposed first by de Goey and co-workers [30] allowed stabilizing adiabatic flat flames using heat loss compensation in order to derive adiabatic burning velocities directly from inlet gas flow rate measurements. The burner head was a perforated 30 mm diameter brass plate. The head was mounted on a mixing chamber enclosed in a thermostatic oil jacket, the temperature of which was set to the desired initial temperature of the fresh gas mixture. The circumference of the burner plate was heated with thermostatic oil set to about 50 K above the temperature of the unburned gas mixture so that the heat gain of the unburned gas mixture from the burner can compensate for the heat loss from the flame to the burner necessary to stabilize the flame. The adiabaticity of the flame was checked by eight type K thermocouples inserted into holes of the burner plate and positioned at different distances and angles from the center to the periphery of the burner. When the temperature profile was flat, it meant that no heat was globally lost or gained by the flame and that the flame became adiabatic with respect to the burner. The adjustment of the flow rate of the gas mixture made it possible to find the appropriate gas velocity, which canceled out the net heat flux so that the radial temperature distribution in the burner plate was uniform. The flow rate at which the net heat flux was zero corresponded to the adiabatic flame burning velocity. The burning velocity of fuel/air mixtures has been investigated under atmospheric pressure for fresh gas temperature 298 K, 358 K, and 398 K and equivalence ration ranging from 0.6 to 1.9. The air was considered as a 21/79 vol. oxygen/nitrogen blend. Gas flow rates were measured using Bronkhorst High-Tech Mass Flow Controllers (MFC). Oxygen and nitrogen were delivered by Messer (purity>99.995%vol.). The uncertainty in the laminar burning velocity can be first attributed to the uncertainty in the mass flow measurements (around 0.5% for each MFC) which can lead to a global uncertainty of 1.5% and around 1% in equivalence ratio. The uncertainty in reading the temperature with thermocouples which could lead to an error of around 0.2 cm/s in the laminar burning velocity, and to errors due directly to flame distortions, such as edge effects (estimated around 0.2 cm/s). In the case of very rich mixtures, the change in the curvature of the temperature profile with the gas flow.

RESULTS AND DISCUSSION

The carbon, hydrogen, and oxygen atom balances were checked in all flames. The quantified mole fraction of argon allowed taking into account the change in the total mole number along the flame profiles. The difference between inlet and outlet is ~3-4 % for C, ~5-9 % for O and H. About 40 to 60 species were identified and quantified in the THF, THP and MTHF flames, respectively. Only selected important species will be presented and discussed in the following

paragraphs. Figures 2 to 8 present the mole fraction profiles of chemical species (major and intermediate) as a function of distance above the burner h . The reaction zone peaks at $\sim 1-3$ mm above the burner.

Figure 2 shows the major species profiles, including reactants, diluent (Ar), and main products (CO , CO_2 , H_2O , and H_2) in THF, MTHF and THP flames. This figure shows that THF and THP are completely consumed at height 2.0 mm, but at height 2.5 mm for MTHF. A significant mole fraction of O_2 ($\sim 2 \times 10^{-2}$) remains in the post flame region. The main final products are, to a large extent, CO_2 and H_2O . The profiles of CO display a marked maximum at height 2.5 mm ($\sim 9.5 \times 10^{-2}$) in the THF flame and at height 3.0 mm (8.7×10^{-2}) in the MTHF flame. It can be seen that there is also a remaining mole fraction of CO ($\sim 5 \times 10^{-2}$) and H_2 (1 to 1.5×10^{-2}) in the post flame region. The maximum mole fraction of the main products is quite comparable for the different ether flames. This observation is logical with the similar C/O and C/H ratios in flames conditions (see Table 1). The major as well as intermediate species profiles show that the THF and THP flame fronts are closer to the burner compared to the MTHF flame, reflecting a higher adiabatic burning velocities of THF (37,3, 42,2 et 41,4 cm s^{-1} respectively for MTHF, THP and THF at $\phi=1$ and 298 K, see below).

A comparison of the evolution of the mole fraction of CO as a function of the conversion of the fuel is presented in Figure 3 and shows that the mole fraction of this product follows the following order: $\text{CO (THF)} \sim \text{CO (THP)} > \text{CO (MTHF)}$; the process of CO elimination from the ether fuel looks very similar for THF and THP and the presence of a methyl group in the MTHF prevents this process. A comparison with flames of furan fuels shows that CO is produced in a lower amount in flames of saturated cyclic ethers (THF, MTHF and THP) than in flames of unsaturated cyclic ethers of the furan family [31]. This difference can be explained by the following reasons. First, CO is produced from several important routes of unsaturated ether consumption in furan fuel flames. In addition, the C/O and C/H ratios of ether flames (0.33 and 0.5 respectively) are lower than those of furan flames (C/O = 0.38-0.40 and C/H = 0.75-1).

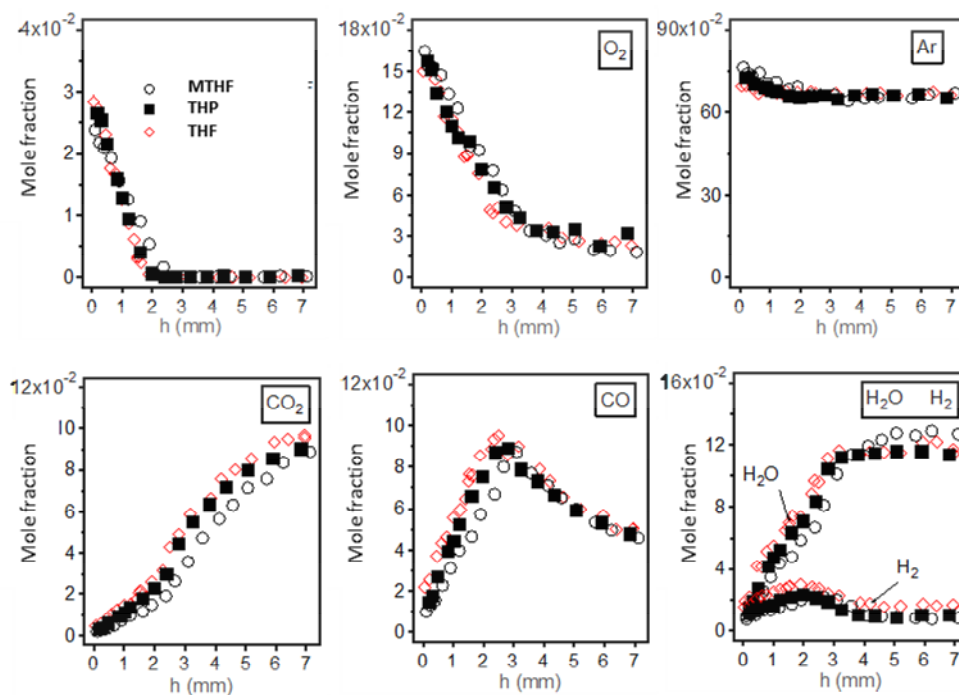


Figure 2. Profile of major species as a function of the height above the burner

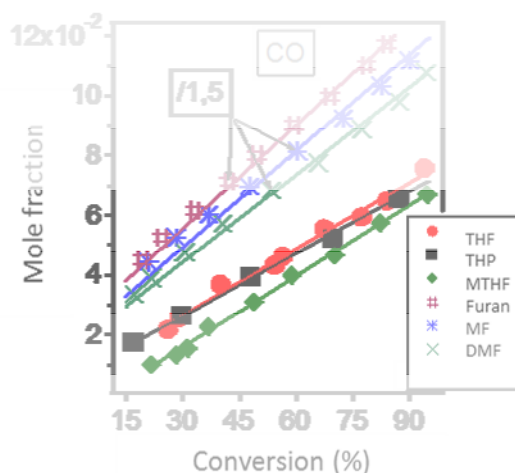


Figure 3. Evolution of the mole fraction of CO as a function of the conversion of the fuel.

The mole fraction profiles of the C₁-C₂ hydrocarbon intermediates including methane (CH₄), ethane (C₂H₆), ethylene (C₂H₄) and acetylene (C₂H₂) are shown in Figure 4. Results in an ethanol flame are reported for comparison. Ethylene is the most abundant intermediate quantified in flames of saturated cyclic ethers (peak mole fraction of 11-12×10⁻³). Ethylene was detected with a lower mole fraction in the ethanol flame (peak mole fraction of 5×10⁻³). This species is an important primary product in the combustion of these ethers and ethanol as shown. On the other hand, acetylene was the most abundant intermediate formed in the flames of unsaturated cyclic ethers [31]. Figure 4 shows that the C₂ intermediates are present in equivalent amounts for the flames of MTHF, THP and THF. Methane is produced in equivalent amounts in flames of THP, THF and ethanol (maximum fraction 2.5×10⁻³), but in a

higher amount in the MTHF flame (peak mole fraction 3.7×10^{-3}). This clearly reflects the influence of the CH_3 group in the MTHF molecule on CH_4 formation.

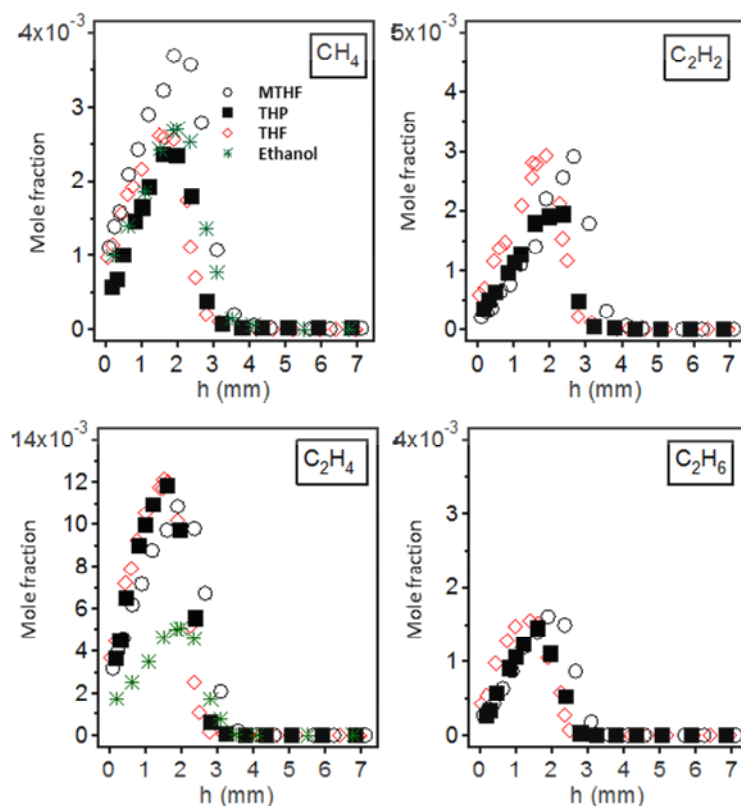


Figure 4. C_1 - C_2 hydrocarbon intermediates

Figure 5 shows the mole fraction profiles of selected non-oxygenated C_5 - C_6 intermediates, which are pollutants and soot precursors. This figure shows that these species are formed in small amounts (less than 50 ppm). These compounds are produced in higher amounts in the flames of MTHF and THP than in the flame of THF, indicating that the fuels containing 5 carbon atoms (MTHF and THP) promote the formation of these large compounds. It is interesting to note that 2-pentene is the most abundant of the two isomers of C_5H_{10} (1-pentene and 2-pentene) in the flames of MTHF and THP, while 1-pentene is most abundant in the flame of THF. 1,3-Cyclopentadiene is produced in a higher quantity in the flame of MTHF (12 ppm) than in the flames of THP (2 ppm) and THF (trace). Benzene (C_6H_6) is relatively little produced (less than 10 ppm) in these three flames; the combustion of these saturated cyclic ethers has a low tendency to form soot. Note that a reverse trend was noted for the combustion of unsaturated cyclic ethers of the furan family [31][32].

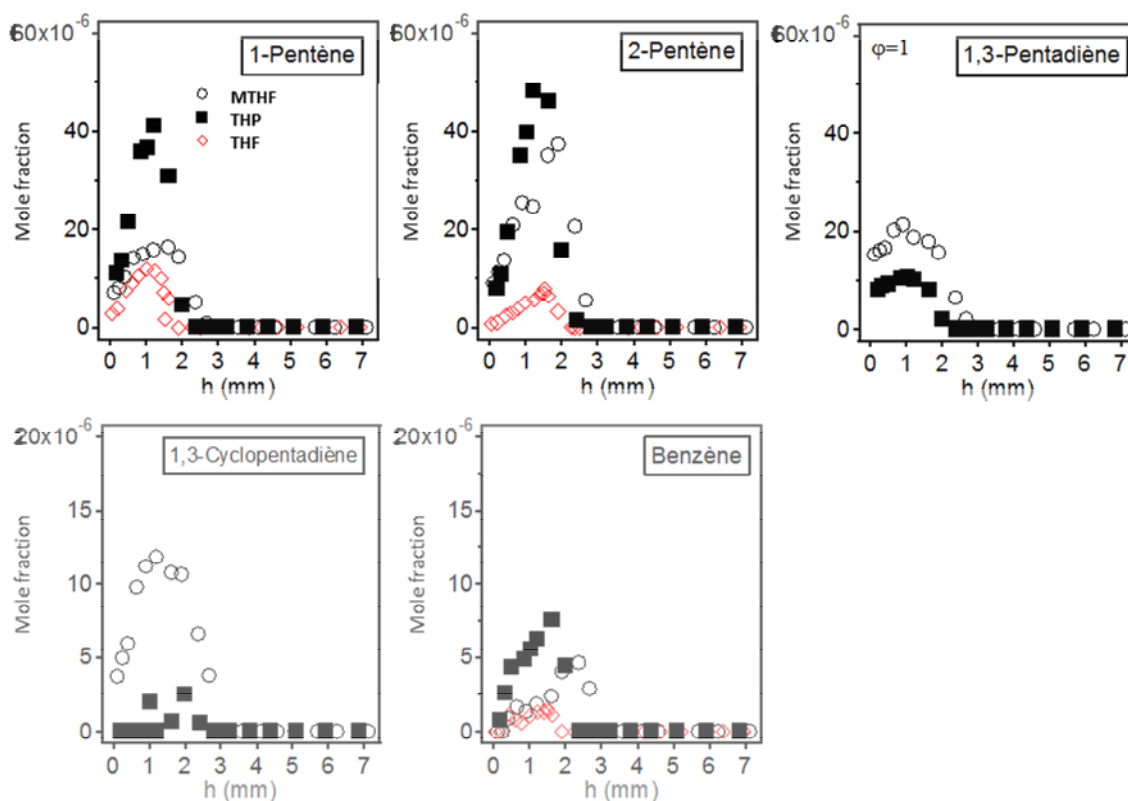


Figure 5. C₅-C₆ hydrocarbon intermediates

The mole fraction profiles of some oxygenated intermediates are shown in Figures 6. The most abundant species among the oxygenated intermediates is formaldehyde (HCHO) for flames of MTHF, THP and THF, while acetaldehyde (CH₃CHO) is the most important of the oxygenated intermediates formed in the ethanol flame. The mole fraction profiles of formaldehyde are relatively similar for the three flames of MTHF, THF and ethanol (maximum around 3×10^{-3}). On the other hand, this compound is produced in a larger amount in the flame of THP (peak mole fraction of 4.5×10^{-3}). Note that this compound is a primary product of the combustion of these four fuels. Acetaldehyde is also a primary product of the oxidation of MTHF, THF and ethanol. This compound was measured with mole fractions of 1.2×10^{-3} , 0.7×10^{-3} and 0.25×10^{-3} respectively in the flames of MTHF, THP and THF. These values are very low compared to that obtained in flame of ethanol (5.5×10^{-4}). Acetaldehyde is therefore a specific product of the combustion of ethanol: H-atom abstractions on the α -position of OH in ethanol yield the α -hydroxyethyl radical CH₃CHOH, which reacts mainly by oxidation and β -scission of the O-H bond to form the acetaldehyde. In the case of the MTHF flame, acetaldehyde can be produced by pulling out a hydrogen atom at the C₄ position giving the 2-methyltetrahydrofuran-4-yl radical (MTHF-yl-4). The other three oxygenated C₂ intermediates detected are dimethyl ether (DME, CH₃OCH₃), ketene (CH₂CO) and ethylene oxide (not shown). DME profiles appear to be similar for the four flames (MTHF, THP, THF and ethanol). On the other hand, the formation of the ketene is different according to the different flames. The mole fraction of this compound decreases from the flame of THF to that of MTHF and that of THP. The formation of this compound depends on the structure of the fuels. In the flames of THF and MTHF, the resonance-stabilized radical

CH_2CHO , which produces ketene, is formed by important consumption routes of the reactants: H-atom abstractions in alpha position of the O-atom), followed by the β -scission, whereas CH_2CHO radical does not appear directly in the decomposition pathways of THP.

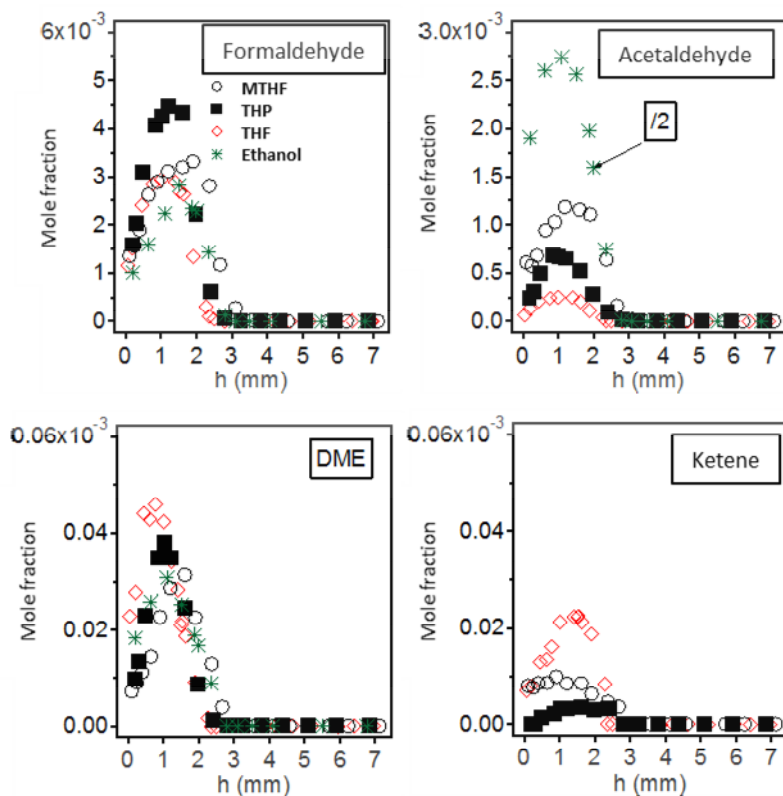


Figure 6. C_1 - C_2 oxygenated intermediates

Figure 7 shows the mole fraction profiles of the C_3 oxygenated intermediates: two isomers of $\text{C}_3\text{H}_6\text{O}$ (acetone and propanal) and acrolein (containing a proportion of furan). This figure shows that acetone is produced much more in the MTHF flame (with a peak mole fraction of 10×10^{-5}) than in the other flames, while acrolein is produced much more in the flame of THP (peak mole fraction of 70×10^{-5}). Acrolein can be produced from the H-abstraction of the hydrogen atom alpha and beta positions in THP followed by a few β -scissions. In the case of acetone, this compound is often formed by combinations between CH_3CO and CH_3 radicals or between a hydrogen atom and CH_3COCH_2 radical. Because of the presence of a methyl group, this CH_3COCH_2 radical may derived directly from MTHF via the formation of the 2-methyltetrahydrofuran-2-yl radical followed by a decomposition by β -scission. Acetone is consequently produced with a higher mole fraction in the MTHF flame than in the other flames.

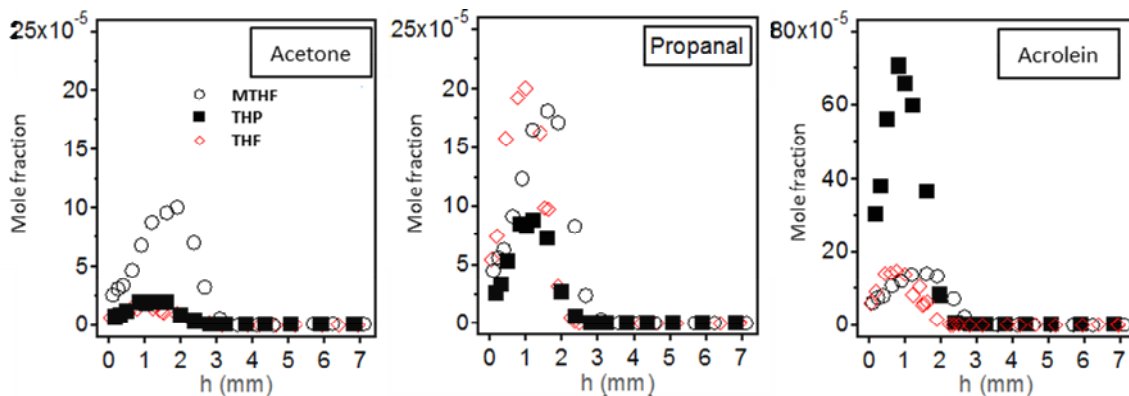


Figure 7. C₃ oxygenated intermediates

Figure 8 compares the profiles of two selected pollutants, benzene and formaldehyde, produced in the 1-pentanol flame to the amount obtained in the flames of cyclic ethers. It appears that the alcohol, as ethanol, produced much more formaldehyde than the ethers. This is due mainly to the H-atom abstractions from the hydroxyl group. The decomposition of the alkoxy radical yields the aldehyde. On the other hand, the linear saturated alcohol produced less unsaturated intermediates than cyclic ethers and limits the formation of aromatic rings.

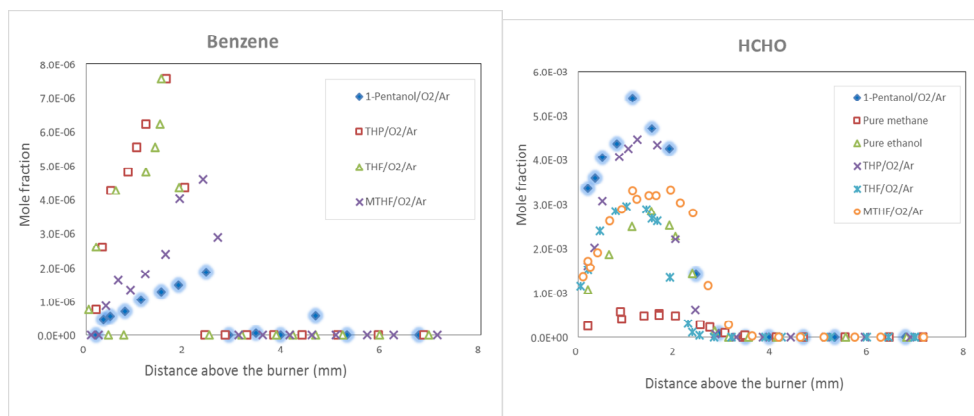


Figure 8. Comparison of benzene and formaldehyde profiles in 1-pentanol and ether flames.

The laminar burning velocities of the studied compounds in air have been measured at 298K, 358K, and 398K as a function of the equivalence ratio and are compared in Figure 4. It has been found that the presence of a methyl group in the 2-methyltetrahydrofuran reduces the laminar burning velocity compared to tetrahydrofuran. The opposite effect is observed when the ring of the cyclic compound has one more carbon atom, as in tetrahydropyran. In this case, the laminar burning velocity measured under the same conditions is higher. Laminar burning velocities of 1-pentanol have been measured at room temperature and are much higher than that of the ethers with the same carbon number.

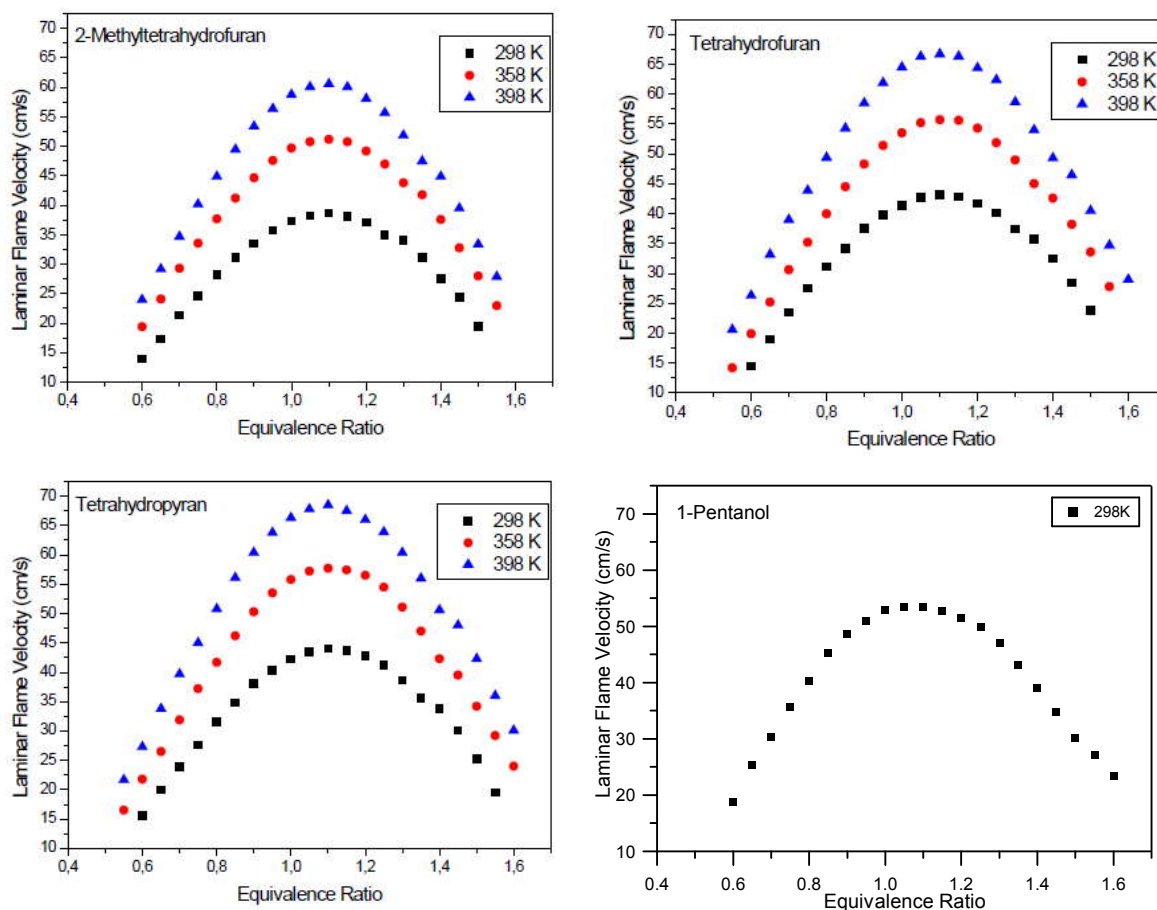


Figure 9. Burning velocities of saturated ethers and 1-pentanol

CONCLUSION

This paper presents experimental results about the chemical structure of low-pressure laminar premixed flame of THF MTHF, THP, and 1-pentanol, as well as their burning velocities in air. The temperature and mole fraction profiles of about 36-45 species (including ~12-19 oxygenated intermediates) were measured. The results show that the mole fraction of the intermediates varies strongly according to the structure of the fuel, in particular for oxygenated compounds. Ethylene is the most abundant intermediate, and formaldehyde is the most abundant oxygen intermediate. Acetaldehyde is produced in a much smaller amount in flames of cyclic ethers than in flames of alcohols. The flame of THP has a strong tendency to produce formaldehyde and acrolein. For all products, the mole fraction profiles of the non-oxygenated (<math><C_4</math>) light compounds obtained in the flames of symmetrical cyclic ethers (THF and THP) appear to be similar. Due to the presence of the methyl group, the chemistry of the combustion of MTHF has some differences compared to THF and THP. The cyclic ethers containing 5 carbon atoms (MTHF and THP) favor the formation of heavier compounds much more than the linear alcohol. Nevertheless, soot precursors are produced in very small amounts in the flames of these saturated cyclic ethers.

References

- [1] Wallington, T. J., W. O. Siegl, R. Liu, Z. Zhang, R. E. Huie, and M. J. Kurylo, 1990, The atmospheric reactivity of alpha-methyltetrahydrofuran: *Environmental Science & Technology*, 24, 1596.
- [2] Yang, W., and A. Sen, 2010, One-Step Catalytic Transformation of Carbohydrates and Cellulosic Biomass to 2,5-Dimethyltetrahydrofuran for Liquid Fuels: *ChemSusChem*, 3, 97.
- [3] Lange, J.-P., E. van der Heide, J. van Buijtenen, and R. Price, 2012, Furfural—A Promising Platform for Lignocellulosic Biofuels: *ChemSusChem*, 1, 150.
- [4] Tran, L. S., B. Sirjean, P.A. Glaude, R. Fournet, and F. Battin-Leclerc, 2012, Progress in detailed kinetic modeling of the combustion of oxygenated components of biofuels: *Energy*, 43, 4.
- [5] E. Christensen, J. Yanowitz, M. Ratcliff, R. L. McCormick, 2011, Renewable Oxygenate Blending Effects on Gasoline Properties, *Energy Fuels*, 25, 4723.
- [6] J. Campos-Fernandez, J. M. Arnal, J. Gomez, N. Lacalle, M. Pilar Dorado, 2013. Performance tests of a diesel engine fueled with 1-pentanol/diesel fuel blends, *Fuel*, 107, 866
- [7] Rudolph, T. W., and J. J. Thomas, 1988, NO_x, NMHC and CO emissions from biomass derived gasoline extenders, *Biomass*, 16, 33.
- [8] Leppard, W. R., 1987, The autoignition chemistry of n-butane: an experimental study: *SAE transactions*, 96, 934.
- [9] Herbinet, O., S. Bax, P. A. Glaude, V. Carre, and Frederique Battin-Leclerc, 2011, Mass spectra of cyclic ethers formed in the low-temperature oxidation of a series of n-alkanes. *Fuel*, 90, 528.
- [10] Herbinet, O., Frederique Battin-Leclerc, et al., 2011, Detailed product analysis during the low temperature oxidation of n-butane. *Physical Chemistry Chemical Physics*, 13, 296.
- [11] Klute, C. H., and W. D. Walters, 1946, The Thermal Decomposition of Tetrahydrofuran: *Journal of the American Chemical Society*, 68, 506.
- [12] McDonald, G., N. M. Lodge, and W. D. Walters, 1951, The effect of added gases upon the thermal decomposition of tetrahydrofuran: *Journal of the American Chemical Society*, 73, no. 4, p. 1757–1760.
- [13] Lifshitz, A., M. Bidani, and S. Bidani, 1986, Thermal reactions of cyclic ethers at high temperatures. 2. Pyrolysis of tetrahydrofuran behind reflected shocks: *Journal of Physical Chemistry*, 90, 3422–3429.
- [14] Molera, M. J., A. Couto, and J. A. Garcia-Dominguez, 1988, Gas phase oxidation of tetrahydrofuran: *International Journal of Chemical Kinetics*, 20, 673–685.
- [15] Leppard, W. R., 1991, Autoignition chemistries of octane-enhancing ethers and cyclic ethers: A motored engine study. *SAE Transactions*, 100, 589–604.
- [16] Dagaut, P., M. McGuinness, J.M. Simmie, and M. Cathonnet, 1998, The Ignition and Oxidation of Tetrahydrofuran. *Experiments and Kinetic Modeling: Combustion Science and Technology*, 135, 3–29.
- [17] Kasper, T., A. Lucassen, A. W. Jasper, W. Li, P. R. Westmoreland, K. Kohse-Höinghaus, B. Yang, J. Wang, T. A. Cool, and N. Hansen, 2011, Identification of Tetrahydrofuran

- Reaction Pathways in Premixed Flames. *Zeitschrift für Physikalische Chemie*, 225, 1237–1270.
- [18] Simmie, John M., 2012, Kinetics and Thermochemistry of 2,5-Dimethyltetrahydrofuran and Related Oxolanes: Next Next-Generation Biofuels. *Journal of Physical Chemistry A*, 116, 4528–4538.
- [19] Verdicchio, M., B. Sirjean, L.S. Tran, P.A. Glaude, F. Battin-Leclerc. 2015. Unimolecular Decomposition of Tetrahydrofuran: Carbene vs. Diradical Pathways. *Proceedings of the Combustion Institute*, 35, 533-541 (2015)
- [20] Lizardo-Huerta, J.C., B. Sirjean, P.A. Glaude, R. Fournet. 2017. Pericyclic Reactions in Ether Biofuels. *Proceedings of the Combustion Institute*, 36, 569-576 (2017).
- [21] C. Tang, L. Wei, X. Man, J. Zhang, Z. Huang, C. K. Law, 2013, High temperature ignition delay times of C5 primary alcohols, *Combust. Flame*, 160, 520-529.
- [22] K. A. Heufer, J. Bugler, et H. J. Curran, 2013, A comparison of longer alkane and alcohol ignition including new experimental results for n-pentanol and n-hexanol , *Proc. Combust. Inst.*, 34, 511-518.
- [23] C. Togbe, F. Halter, F. Foucher, C. Mounaim-Rousselle, P. Dagaut, 2011, Experimental and detailed kinetic modeling study of 1-pentanol oxidation in a JSR and combustion in a bomb », *Proc. Combust. Inst.*, 33, 367-374.
- [24] Q. Li, E. Hu, X. Zhang, Y. Cheng, Z. Huang, 2013, Laminar Flame Speeds and Flame Instabilities of Pentanol Isomer-Air Mixtures at Elevated Temperatures and Pressures, *Energy Fuels*, 27, 1141-1150.
- [25] L. Zhao, L. Ye, F. Zhang, L. Zhang, 2012, Thermal Decomposition of 1-Pentanol and Its Isomers: A Theoretical Study, *J. Phys. Chem. A*, 116, 9238-9244.
- [26] Pousse, E., P. A. Glaude, R. Fournet, and F. Battin-Leclerc, 2009, A lean methane premixed laminar flame doped with components of diesel fuel I. n-Butylbenzene: *Combustion and Flame*, 156, 954–974.
- [27] P. Dirrenberger, H. Le Gall, R. Bounaceur, O. Herbinet, P.-A. Glaude, A. Konnov, F. Battin-Leclerc, 2011, Measurements of laminar flame velocity for components of natural gas, *Energ. Fuel*. 25, 3875-3884.
- [28] P. Dirrenberger; P-A. Glaude; R. Bounaceur; H. Le Gall; A. Pires da Cruz; A. Konnov; F. Battin-Leclerc, Laminar burning velocity of gasolines with addition of ethanol, 2014, *Fuel* 115, 162–169.
- [29] P. Dirrenberger, H. Le Gall, R. Bounaceur, P.-A. Glaude, F. Battin-Leclerc, 2015, Measurements of Laminar Burning Velocities above Atmospheric Pressure Using the Heat Flux Method. Application to the Case of n-Pentane, *Energy & Fuels* 29, 398.
- [30] L.H.P. De Goey, A. Van Maaren, R.M. Quax, 1993, Stabilization of adiabatic premixed laminar flames on a flat flame burner, *Combust. Sci. Technol.* 92, 201-207.
- [31] C. Togbé, L.S. Tran, D. Liu, D. Felsmann, P. Oßwald, P.A. Glaude, B. Sirjean, R. Fournet, F. Battin-Leclerc, K. Kohse-Höinghaus, 2014. Combustion chemistry and flame structure of furan group biofuels using molecular-beam mass spectrometry and gas chromatography - Part III: 2,5-Dimethylfuran. *Combustion and Flame*, 161, 780-797.

- [32] L.S. Tran, B. Sirjean, P.A. Glaude, K. Kohse-Höinghaus, F. Battin-Leclerc. 2015. Influence of substituted furans on the formation of polycyclic aromatic hydrocarbons in flames. *Proceedings of the Combustion Institute*, 35, 1735-1743.